

On the Consistency of Non-Stationary Multipath Fading Channels with Respect to the Average Doppler Shift and the Doppler Spread

Matthias Pätzold

University of Agder

Faculty of Engineering and Science

NO-4898 Grimstad, Norway

Email: matthias.paetzold@uia.no

Carlos A. Gutierrez

Universidad Autonoma de San Luis

San Luis Potosi 78290, Mexico

Email: cagutierrez@ieee.org

Néji Youssef

Ecole Supérieure des Communications de Tunis

Cité El Ghazala, 2083 Ariana, Tunis, Tunisia

Email: neji.youssef@supcom.rnu.tn

Abstract—This paper is concerned with the consistency of non-stationary multipath fading channels. We introduce conditions under which a channel model is consistent w.r.t. the average Doppler shift and the Doppler spread. The conditions are applied to two classes of non-stationary channel models. The first class, which is termed Class \mathcal{A} , is characterized by channel models based on an integral relationship between the path phases and the associated time-variant Doppler frequencies. The second class of models, called the Class \mathcal{B} models, emerges from standard sum-of-cisoids (SOC) models by replacing the time-independent Doppler frequencies by time-dependent Doppler frequencies. It is shown that the Class \mathcal{A} models fulfil the consistency conditions, while the Class \mathcal{B} models are inconsistent. The majority of existing non-stationary channel models with time-dependent Doppler frequencies fall in the Class \mathcal{B} category, meaning that these models suffer from a lack of physical soundness. The importance of the paper comes from the fact that it provides guidelines for the design of consistent and physically reasonable non-stationary channel models.

I. INTRODUCTION

In the past, the modelling of multipath fading channels has concentrated on the characterization of the temporal, frequency, and spatial behaviour of mobile radio channels assuming that the channel is wide-sense stationary. The wide-sense stationary assumption, however, is only fulfilled during very short, so-called stationary intervals, which have been investigated, e.g., in [1]–[3]. If a multipath fading channel is observed over time periods larger than the stationary interval, then the channel develops signs of non-stationarity. The underlying cause of non-stationarity can have a variety of reasons. One reason can be that the mobile station (MS) changes its speed and/or driving direction, or that the angles of arrival (AOAs) are changing with time during the movement of the MS. Another reason can be that some propagation paths are suddenly blocked by obstacles or that new propagation paths emerge along the course of the MS.

A non-stationary channel model that accounts for the impact of the MS's acceleration on the statistics of Rayleigh fading channels has been presented in [4], [5]. A more general non-stationary channel model that captures the effects of both speed variations and changes of the angle of motion (AOM)

was proposed in [6]. Recently, the work in [6] has been extended in [7] towards the modelling of non-stationary mobile-to-mobile double Rayleigh fading channels. The models in [4]–[7] have in common that they originate from stationary plane wave models or sum-of-cisoids (SOC) models in which the time-independent Doppler frequencies have been replaced by time-variant Doppler frequencies. The same procedure has been applied in [8] and [9] to model non-stationary channels.

In this paper, we propose a class of channel models, referred to as Class \mathcal{B} models, that includes the channel models in [4]–[9] as special cases. It is shown that all non-stationary channel models of Class \mathcal{B} are inconsistent in the sense that the average Doppler shift of the multipath components is unequal to the average Doppler shift obtained from the time-variant autocorrelation function (ACF) of the complex channel gain. It is also shown that the same property holds for the Doppler spread. A solution of the inconsistency problem is shown by computing the path phases by integrating over the associated time-variant Doppler frequencies. This motivates us to introduce a new class (Class \mathcal{A}) of non-stationary channel models, that is shown to be consistent w.r.t. the average Doppler shift and the Doppler spread. The proposed Class \mathcal{A} models allow studying the effects of speed variations, AOM variations, and AOA variations with different degrees of complexity. As a side benefit of our results, we propose a simple but accurate method for the computation of the stationary intervals.

The remainder of this paper is organized as follows. Section II introduces the considered non-stationary multipath propagation scenario. Section III derives models for the time-variant channel parameters. Section IV defines the term *consistency* in the context of this paper. Two classes of non-stationary channel models are described in Section V. Section VI presents a selection of numerical results to illustrate the main findings of this study. Finally, the conclusion is drawn in Section VII.

II. THE MULTIPATH PROPAGATION SCENARIO

The considered multipath propagation scenario consists of a fixed base station (BS) (transmitter) and an MS (receiver) that moves with time-variant velocity $\vec{v}(t)$. Both the BS and the MS

© 2017 IEEE. Personal use of this material is permitted. Permission from IEEE must be obtained for all other uses, in any current or future media, including reprinting/republishing this material for advertising or promotional purposes, creating new collective works, for resale or redistribution to servers or lists, or reuse of any copyrighted component of this work in other works.”

DOI 10.1109/WCNC.2017.7925517

are equipped with omnidirectional antennas. It is supposed that the BS antenna is unobstructed by objects, whereas the MS antenna is surrounded by a large number of N fixed scatterers S_n ($n = 1, 2, \dots, N$). Furthermore, we assume that the line-of-sight component is blocked. At time $t = 0$, the MS is located at the origin $(0, 0)$ of the xy -plane as shown in Fig. 1. This figure depicts only the location of the n th local scatterer S_n relative to the MS, while the other $N - 1$ local scatterers have been removed for visual clarity. The local scatterers S_n are fixed and their positions (x_n, y_n) are known for all $n = 1, 2, \dots, N$. The distance between the scatterer S_n and the origin $(0, 0)$ is determined by $r_n = \sqrt{x_n^2 + y_n^2}$. As indicated in Fig. 1, the MS moves with velocity $\vec{v}(t)$ along a path (---) described by the coordinates $x(t)$ and $y(t)$. Along the course of the path, the AOA $\alpha_n(t)$ seen from the position $(x(t), y(t))$ of the MS varies with time t . The initial AOA α_n , shown in Fig. 1, is the AOA $\alpha_n(t)$ at $t = 0$, i.e., $\alpha_n = \alpha_n(0)$.

If an MS moves with known velocity $\vec{v}(t)$ in a deterministic propagation area characterized by fixed scatterers S_n at known locations (x_n, y_n) , then the initial AOAs α_n are constants and the time-variant AOAs $\alpha_n(t)$ are deterministic processes for all $n = 1, 2, \dots, N$. This contrasts with random propagation areas, in which the scatterers S_n are randomly distributed, implying that the initial AOAs α_n are random variables and the time-variant AOAs $\alpha_n(t)$ are stochastic processes. In this paper, we consider a deterministic propagation area with fixed scatterers S_n at known locations (x_n, y_n) .

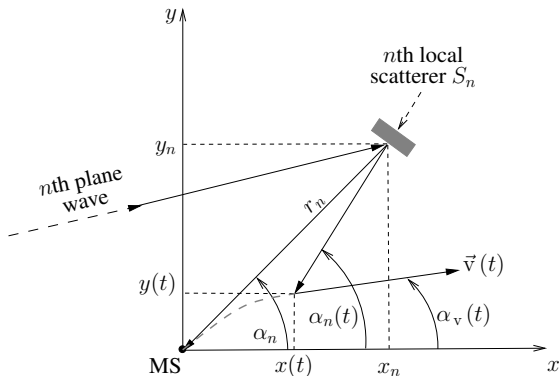


Fig. 1: A multipath propagation scenario in which the MS travels along a path (---) with time-variant velocity $\vec{v}(t)$.

III. MODELLING THE TIME-VARIANT CHANNEL PARAMETERS

A. Modelling the Time-Variant Velocity

In the considered multipath propagation scenario, the MS can change its velocity $\vec{v}(t)$. It is known from kinematics that the velocity $\vec{v}(t)$ is a vector, which can be represented in polar coordinates by $\vec{v}(t) = v(t) \exp\{j\alpha_v(t)\}$, where the magnitude $v(t) = |\vec{v}(t)|$ is called the speed, and $\alpha_v(t)$ denotes the angle of motion (AOM). A change of the MS's velocity $\vec{v}(t)$ can either be attributed to a change in speed $v(t)$, a change in the AOM $\alpha_v(t)$, or a change in both $v(t)$ and $\alpha_v(t)$. As proper

models for the time-variant speed $v(t)$ and the time-variant AOM $\alpha_v(t)$, we adopt the following expressions from [6]

$$v(t) = v_0 + a_0 t \quad (1)$$

$$\alpha_v(t) = \alpha_v + b_0 t. \quad (2)$$

In (1), v_0 denotes the initial speed at $t = 0$, and a_0 is called the acceleration parameter if $a_0 > 0$ or deceleration parameter if $a_0 < 0$. Analogously, in (2), α_v denotes the initial AOM at $t = 0$, and b_0 is called the angular speed. Note that in all other cases in which the speed $v(t)$ and AOM $\alpha_v(t)$ do not change linearly with time t , the expressions in (1) and (2) can be considered as first-order Taylor series approximations of any arbitrary functions $v(t)$ and $\alpha_v(t)$ around $t = 0$, respectively.

B. Modelling the Time-Variant AOAs

The AOA $\alpha_n(t)$ is defined as the angle between the propagation direction of the n th incident wave and the x -axis. With reference to Fig. 1, the AOA $\alpha_n(t)$ can be expressed as

$$\alpha_n(t) = \arctan\left(\frac{y_n - y(t)}{x_n - x(t)}\right) \quad (3)$$

for $n = 1, 2, \dots, N$, where the positions $x(t)$ and $y(t)$ of the MS at time t can be obtained from

$$x(t) = \int_0^t v(z) \cos(\alpha_v(z)) dz \quad (4)$$

and

$$y(t) = \int_0^t v(z) \sin(\alpha_v(z)) dz \quad (5)$$

respectively. By developing the AOA $\alpha_n(t)$ in a first-order Taylor series around $t = 0$, we can approximate the nonlinear function $\alpha_n(t)$ in (3) by a linear function of time t as follows

$$\alpha_n(t) \approx \alpha_n + \gamma_n t \quad (6)$$

where

$$\alpha_n = \alpha_n(0) = \arctan\left(\frac{y_n}{x_n}\right) \quad (7)$$

$$\gamma_n = \left.\frac{d}{dt}\alpha_n(t)\right|_{t=0} = \frac{v_0}{r_n} \sin(\alpha_n - \alpha_v). \quad (8)$$

The approximation error caused by retaining only the first two terms of the Taylor series in (6) influences the time-variant Doppler shift and the time-variant Doppler spread. The effect of this approximation error will be analyzed in Section VI.

C. Modelling the Time-Variant Doppler Frequencies

According to the Doppler effect, the n th received multipath component experiences a time-variant Doppler shift $f_n(t)$ if the MS changes its velocity $\vec{v}(t)$ over time t . This time-variant Doppler shift can accurately be modelled as

$$f_n(t) = f_{\max}(t) \cos(\alpha_n(t) - \alpha_v - b_0 t) \quad (9)$$

for all $n = 1, 2, \dots, N$, where $\alpha_n(t)$ is given by (3) and

$$f_{\max}(t) = \frac{f_0}{c_0} v(t) = \frac{f_0}{c_0} (v_0 + a_0 t) \quad (10)$$

denotes the time-variant maximum Doppler frequency. In (10), f_0 and c_0 designate the carrier frequency and the speed of light, respectively. Note that (9) presents the exact solution for $f_n(t)$ if $\alpha_n(t)$ according to (3) is used, and if the speed $v(t)$ and AOM $\alpha_n(t)$ are linearly varying with time t . A simpler nonlinear model can be obtained for the time-variant Doppler shift $f_n(t)$ by using (6) instead of (3), which allows us to represent $f_n(t)$ as

$$f_n(t) = f_{\max}(t) \cos[\alpha_n - \alpha_v + (\gamma_n - b_0)t]. \quad (11)$$

A third and even less complex Doppler frequency model can be obtained by developing the expression in (9) in a Taylor series around $t = 0$ and retaining only the first two terms. This results in the linear Doppler frequency model

$$f_n(t) = f_n + k_n t \quad (12)$$

where

$$f_n = f_n(0) = f_{\max} \cos(\alpha_n - \alpha_v) \quad (13)$$

$$k_n = \left. \frac{d}{dt} f_n(t) \right|_{t=0} = f_{\max} \left[\frac{a_0}{v_0} \cos(\alpha_n - \alpha_v) + (b_0 - \gamma_n) \sin(\alpha_n - \alpha_v) \right] \quad (14)$$

with f_{\max} being the initial maximum Doppler shift defined as $f_{\max} = f_{\max}(0) = f_0 v_0 / c_0$. Note that k_n can be written as a sum of three terms. The first term accounts for the acceleration (deceleration) of the MS. The second term is due to the change of the direction of motion, and the third term is a result of the changing AOA. Note also that for the stationary case, where $a_0 = 0$, $b_0 = 0$, and $\gamma_n = 0$ hold, all three Doppler frequency models described by (9), (11), and (12) reduce to the well-known expression $f_n(t) = f_n = f_{\max} \cos(\alpha_n - \alpha_v)$ that is exclusively used for the characterization of the Doppler shift in stationary mobile radio channels. The same statement holds if we observe the channel at $t = 0$.

IV. DEFINITION OF CONSISTENCY

This section presents a working definition of the property that a non-stationary multipath channel model is consistent w.r.t. the average Doppler shift and the Doppler spread.

In frequency-nonselctive mobile radio channels, the complex channel gain $\mu_n(t)$ of the received n th multipath component can be described by $\mu_n(t) = c_n \exp\{j\theta_n(t)\}$, where c_n represents the path gain which is real valued, and $\theta_n(t)$ is the associated path phase that is in some way a function of the Doppler frequency $f_n(t)$, i.e., $\theta_n(t) = g(f_n(t))$. We consider sufficiently short observation intervals T_{obs} , such that the path gain c_n does not vary with time $t \in [0, T_{\text{obs}}]$ or the position $(x(t), y(t))$ of the MS on its route. In this case, the instantaneous power of n th multipath component is constant and equals the squared path gain, i.e., $|\mu_n(t)|^2 = c_n^2$. Without

any a priori information on the path phases $\theta_n(t)$, the time-variant average Doppler shift $B_f^{(1)}(t)$ can then be obtained by computing the sum of all power-weighted Doppler shifts normalized onto the total received power of all multipath components according to

$$B_f^{(1)}(t) = \frac{\sum_{n=1}^N c_n^2 f_n(t)}{\sum_{n=1}^N c_n^2}. \quad (15)$$

The equation above holds for all given gains c_n and time-variant Doppler frequencies $f_n(t)$, no matter if we use the exact solution in (9) or the approximations presented in (11) or (12).

Analogously, we can compute the time-variant Doppler spread $B_f^{(2)}(t)$ of a non-stationary multipath channel with given path gains c_n and time-variant Doppler frequencies $f_n(t)$ by means of

$$B_f^{(2)}(t) = \sqrt{\frac{\sum_{n=1}^N c_n^2 f_n^2(t)}{\sum_{n=1}^N c_n^2} - \left(B_f^{(1)}(t)\right)^2}. \quad (16)$$

Alternatively, we can compute the time-variant Doppler shift $B_\mu^{(1)}(t)$ and the time-variant Doppler spread $B_\mu^{(2)}(t)$ of the complex channel gain $\mu(t) = \sum_{n=1}^N \mu_n(t)$ of all N multipath components by means of the time-dependent ACF

$$\mathcal{R}_\mu(\tau, t) = E \left\{ \mu \left(t + \frac{\tau}{2} \right) \mu^* \left(t - \frac{\tau}{2} \right) \right\} \quad (17)$$

where $E\{\cdot\}$ and $(\cdot)^*$ denote the expectation operator and the complex conjugation operator, respectively. This alternative approach leads to

$$B_\mu^{(1)}(t) = \frac{1}{2\pi j} \frac{\dot{\mathcal{R}}_\mu(0, t)}{\mathcal{R}_\mu(0, t)} \quad (18)$$

and

$$B_\mu^{(2)}(t) = \frac{1}{2\pi} \sqrt{\left(\frac{\dot{\mathcal{R}}_\mu(0, t)}{\mathcal{R}_\mu(0, t)} \right)^2 - \frac{\ddot{\mathcal{R}}_\mu(0, t)}{\mathcal{R}_\mu(0, t)}} \quad (19)$$

where $\dot{\mathcal{R}}_\mu(0, t)$ ($\ddot{\mathcal{R}}_\mu(0, t)$) denotes the first (second) derivative of $\mathcal{R}_\mu(\tau, t)$ w.r.t. the time separation variable τ at $\tau = 0$.

Definition: A non-stationary multipath channel model is said to be consistent w.r.t. the Doppler shift if the condition $B_f^{(1)}(t) = B_\mu^{(1)}(t)$ is fulfilled for all t . Analogously, we say that a channel model is consistent w.r.t. the Doppler spread if the identity $B_f^{(2)}(t) = B_\mu^{(2)}(t)$ holds for all t .

V. TWO CLASSES OF CHANNEL MODELS

A. Channel Models of Class A

The basic idea of deriving Class A channel models is to invoke the phase-frequency relationship [10, Eq. (1.3.40)]

$$f_n(t) = \frac{1}{2\pi} \frac{d\theta_n(t)}{dt} \quad (20)$$

for all $n = 1, 2, \dots, N$. From (20), the path phase $\theta_n(t)$ can then be derived as follows

$$\begin{aligned}\theta_n(t) &= 2\pi \int_{-\infty}^t f_n(z) dz \\ &= 2\pi \int_{-\infty}^0 f_n(z) dz + 2\pi \int_0^t f_n(z) dz \\ &= \theta_n + 2\pi \int_0^t f_n(z) dz\end{aligned}\quad (21)$$

where $\theta_n = 2\pi \int_{-\infty}^0 f_n(z) dz$ represents the initial phase at $t = 0$, i.e., $\theta_n = \theta_n(0)$. For the reason that the initial phases θ_n are generally unknown, they will be modelled by independent and identically distributed (i.i.d.) random variables with uniform distribution over $(0, \pi]$, i.e., $\theta_n \sim \mathcal{U}(0, 2\pi]$. By using the exact Doppler frequency model in (9), where $\alpha_n(t)$ is given by (3), the integral in (21) has to be solved numerically. However, in case of the nonlinear Doppler frequency model described by (11), the path phases $\theta_n(t)$ can be expressed in closed form as

$$\begin{aligned}\theta_n(t) &= \theta_n + \frac{2\pi f_{\max}(t)}{\gamma_n - b_0} \left\{ \sin[\alpha_n - \alpha_v + (\gamma_n - b_0)t] \right. \\ &\quad \left. - \sin(\alpha_n - \alpha_v) \right\} + \frac{2\pi a_0}{\lambda(\gamma_n - b_0)^2} \\ &\quad \cdot \left\{ \cos[\alpha_n - \alpha_v + (\gamma_n - b_0)t] - \cos(\alpha_n - \alpha_v) \right\}\end{aligned}\quad (22)$$

where $\lambda = c_0/f_0$ is the wavelength. Moreover, for the linear Doppler frequency model introduced in (12), a simple closed-form solution can be obtained for $\theta_n(t)$ in the form of

$$\theta_n(t) = \theta_n + 2\pi \left(f_n t + \frac{k_n t^2}{2} \right).\quad (23)$$

Using (21), the complex channel gain $\mu(t)$ of narrowband multipath fading channel models of Class \mathcal{A} is then defined by

$$\mu(t) = \sum_{n=1}^N c_n e^{j \left(2\pi \int_0^t f_n(z) dz + \theta_n \right)}.\quad (24)$$

Depending on the modelling philosophy and motivation, the path gains c_n and phases θ_n can be random variables or constants, whereas the Doppler frequencies can either be stochastic processes, deterministic processes, random variables or constants. This implies that Class \mathcal{A} models comprise $2 \cdot 4 \cdot 2 = 16$ different types of channel models, whereof one model is deterministic, seven are wide-sense stationary (if certain boundary conditions are satisfied [11]), and eight are non-wide-sense stationary. It is obvious that the statistical properties of the 16 types of channel models are different.

In the following, we focus on the important case that the path gains c_n are constants, the Doppler frequencies $f_n(t)$ are deterministic processes, and the phases θ_n are i.i.d. random

variables. For this case, the time-dependent ACF $\mathcal{R}_\mu(\tau, t)$ can be brought into the following general form after substituting (24) in (17) and averaging over the i.i.d. phases $\theta_n \sim \mathcal{U}(0, 2\pi]$:

$$\mathcal{R}_\mu(\tau, t) = \sum_{n=1}^N c_n^2 e^{j2\pi \int_{t-\tau/2}^{t+\tau/2} f_n(z) dz}\quad (25a)$$

$$= \sum_{n=1}^N c_n^2 e^{j[\theta_n(t+\tau/2) - \theta_n(t-\tau/2)]}.\quad (25b)$$

For the nonlinear Doppler frequency model described by (11), the integral in (25a) can be solved analytically, yielding

$$\begin{aligned}\mathcal{R}_\mu(\tau, t) &= \sum_{n=1}^N c_n^2 \exp \left\{ j2\pi\tau \left\{ f_n(t) \operatorname{sinc} \left[(\gamma_n - b_0) \frac{\tau}{2} \right] \right. \right. \\ &\quad \left. \left. + \frac{a_0}{\lambda(\gamma_n - b_0)} \sin[\alpha_n - \alpha_v + (\gamma_n - b_0)t] \right. \right. \\ &\quad \left. \left. \left\{ \cos \left[(\gamma_n - b_0) \frac{\tau}{2} \right] - \operatorname{sinc} \left[(\gamma_n - b_0) \frac{\tau}{2} \right] \right\} \right\} \right\}\end{aligned}\quad (26)$$

where $f_n(t)$ is given by (11), and $\operatorname{sinc}(\cdot)$ denotes the sinc function, which is defined as $\operatorname{sinc}(x) = \sin(x)/x$.

Furthermore, for the linear Doppler frequency model [see (12)], we obtain

$$\mathcal{R}_\mu(\tau, t) = \sum_{n=1}^N c_n^2 e^{j2\pi f_n(t)\tau}\quad (27)$$

where $f_n(t)$ is given by (12).

Next, we will analyse the time-variant average Doppler shift $B_\mu^{(1)}(t)$ and the time-variant Doppler spread $B_\mu^{(2)}(t)$ of the complex channel gain $\mu(t)$ introduced in (24). Therefore, we substitute (25a) in (18) and (19), which results after some mathematical manipulations in the following expressions (without proof):

$$B_\mu^{(1)}(t) = \frac{\sum_{n=1}^N c_n^2 f_n(t)}{\sum_{n=1}^N c_n^2}\quad (28)$$

$$B_\mu^{(2)}(t) = \sqrt{\frac{\sum_{n=1}^N c_n^2 f_n^2(t)}{\sum_{n=1}^N c_n^2} - \left(B_\mu^{(1)}(t) \right)^2}.\quad (29)$$

A comparison of (28) with (15) and (29) with (16) shows that the consistency condition $B_f^{(i)}(t) = B_\mu^{(i)}(t)$ is fulfilled for all t and $i = 1, 2$. This result shows that Class \mathcal{A} channel models with constant path gains c_n and random phases θ_n are consistent w.r.t. the average Doppler shift and the Doppler spread for any given Doppler frequency function $f_n(t)$.

B. Channel Models of Class \mathcal{B}

The basic idea of deriving Class \mathcal{B} channel models is to start from SOC models [12, Section 4.5] and to replace the time-invariant Doppler frequencies f_n by time-variant Doppler

frequencies $f_n(t)$. According to this idea, the complex channel gain $\mu(t)$ of Class \mathcal{B} narrowband multipath fading channel models can be expressed as

$$\mu(t) = \sum_{n=1}^N c_n e^{j(2\pi f_n(t) \cdot t + \theta_n)}. \quad (30)$$

Taking all combinations of the model parameters $c_n, f_n(t), \theta_n$ into account, which can be constants or random variables, where $f_n(t)$ can be in addition deterministic or stochastic processes, it is obvious that Class \mathcal{B} comprises as many types of channel models as Class \mathcal{A} , namely 16. It is interesting to note that the Class \mathcal{A} and \mathcal{B} models reduce to the SOC model if the Doppler frequencies $f_n(t)$ are time-invariant, i.e., $f_n(t) = f_n$. Replacing f_n by $f_n(t)$ in an SOC model is simple and straightforward, but the main drawback of this procedure is that the resulting Class \mathcal{B} models are inconsistent, as will be shown below.

In analogy to Class \mathcal{A} models, we consider only the important case that the gains c_n are constants, the Doppler frequencies $f_n(t)$ are deterministic processes, and the phases θ_n are i.i.d. random variables. Then, after substituting (30) in (17) and averaging over the i.i.d. phases $\theta_n \sim \mathcal{U}(0, 2\pi]$, the time-dependent ACF $\mathcal{R}_\mu(\tau, t)$ can be expressed in closed form as

$$\begin{aligned} \mathcal{R}_\mu(\tau, t) = & \sum_{n=1}^N c_n^2 e^{j2\pi[f_n(t+\frac{\tau}{2}) - f_n(t-\frac{\tau}{2})]t} \\ & \cdot e^{j2\pi[f_n(t+\frac{\tau}{2}) + f_n(t-\frac{\tau}{2})]\frac{\tau}{2}}. \end{aligned} \quad (31)$$

Substituting (31) in (18) and (19) results in the following closed-form solutions for the time-variant Doppler shift $B_\mu^{(1)}(t)$ and the time-variant Doppler spread $B_\mu^{(2)}(t)$ (without proof):

$$B_\mu^{(1)}(t) = \frac{\sum_{n=1}^N c_n^2 [f_n(t) + \dot{f}_n(t) \cdot t]}{\sum_{n=1}^N c_n^2} \quad (32)$$

$$B_\mu^{(2)}(t) = \sqrt{\frac{\sum_{n=1}^N c_n^2 [f_n(t) + \dot{f}_n(t) \cdot t]^2}{\sum_{n=1}^N c_n^2}} - \left(B_\mu^{(1)}(t)\right)^2. \quad (33)$$

Comparing (32) and (33) with (15) and (16), respectively, shows that $B_f^{(i)}(t) \neq B_\mu^{(i)}(t)$ for $i = 1, 2$, which means that the non-stationary channel model defined in (30) is inconsistent w.r.t. the average Doppler shift and the Doppler spread. This result is not surprising, because it can be shown (without proof) that the Class \mathcal{A} channel models are the only consistent channel models. In other words, the condition imposed by the phase-frequency relationship (20) is necessary and sufficient for the development of consistent channel models.

VI. NUMERICAL RESULTS

This section presents a selection of numerical results to illustrate our main findings of the time-variant average Doppler shift $B_f^{(1)}(t)$ ($B_\mu^{(1)}(t)$) and the time-variant Doppler spread $B_f^{(2)}(t)$ ($B_\mu^{(2)}(t)$) of the Class \mathcal{A} and \mathcal{B} models.

In our numerical study, we have considered a multipath channel consisting of $N = 10$ components. The path gains c_n and initial AOAs $\alpha_n = \alpha_n(0)$ have been computed by means of the extended method of exact Doppler spread (EMEDS) [13], according to which these parameters are given by

$$c_n = \sigma_0 \sqrt{\frac{2}{N}} \quad \text{and} \quad \alpha_n = \frac{2\pi}{N} \left(n - \frac{1}{4}\right) \quad (34)$$

where the parameter σ_0 has been set to unity. The initial phases $\theta_n = \theta_n(0)$ have been considered as the outcomes of a random generator with uniform distribution over the interval $(0, 2\pi]$. The distances r_n between the scatterers S_n and the origin $(0, 0)$ [see Fig. 1] have been set to 50 m for all $n = 1, 2, \dots, N$. Thus, the positions (x_n, y_n) of the scatterers S_n are then determined by $x_n = r_n \cos(\alpha_n)$ and $y_n = r_n \sin(\alpha_n)$. The parameters of the velocity model described by (1) and (2) have been chosen as follows: $v_0 = 3$ km/h, $a_0 = 1.5$ m/s², $\alpha_v = 0$, and $b_0 = \pi/10$ rad/s. Finally, the carrier frequency f_0 has been set to 5.9 GHz, and the observation duration T_{obs} was 5 s. This results in an initial maximum Doppler frequency of $f_{\text{max}}(0) = f_0 v_0 / c_0 = 16.4$ Hz and a finishing maximum Doppler frequency of $f_{\text{max}}(T_{\text{obs}}) = f_0 (v_0 + a_0 T_{\text{obs}}) / c_0 = 164$ Hz.

Fig. 2 shows the graph (—) of the resulting time-variant average Doppler shift $B_f^{(1)}(t)$ according to (15) by using the exact expression for $f_n(t)$ as given by (9). This figure also shows the graph (- -) of $B_f^{(1)}(t) = B_\mu^{(1)}(t)$ for the stationary case that follows when all Doppler frequencies $f_n(t)$ are supposed to be independent of time and fixed to their initial values, i.e., $f_n = f_n(0) = \text{const.} \forall n = 1, 2, \dots, N$.

Next, we evaluate $B_f^{(1)}(t)$ by using the nonlinear and linear Doppler frequency models described by (11) and (12), respectively. The obtained results for $B_f^{(1)}(t)$ have been added to Fig. 2. It can be seen that the nonlinear Doppler frequency model [see (11)] follows the trend of the exact Doppler frequency model closer than the simple linear model [see (12)]. In addition, Fig. 2 includes the graphs of the average Doppler shift $B_\mu^{(1)}(t)$ of the Class \mathcal{A} and Class \mathcal{B} models. The presented results have been obtained for the two classes by evaluating (28) and (32). Fig. 2 shows that the channel models of Class \mathcal{A} fulfil the consistency condition $B_f^{(1)}(t) = B_\mu^{(1)}(t)$, whereas this is not the case for the Class \mathcal{B} models.

Finally, Fig. 3 shows the corresponding results for the time-variant Doppler spreads $B_f^{(2)}(t)$ and $B_\mu^{(2)}(t)$ for the Class \mathcal{A} and \mathcal{B} models. Note that Fig. 3 shows clearly the advantage of all Class \mathcal{A} models, namely that the second consistency condition $B_f^{(2)}(t) = B_\mu^{(2)}(t)$ is also fulfilled, while this is not the case for the Class \mathcal{B} models.

A comparison between the stationary case (f_n constant) and the non-stationary case (f_n time-variant) allows us to introduce

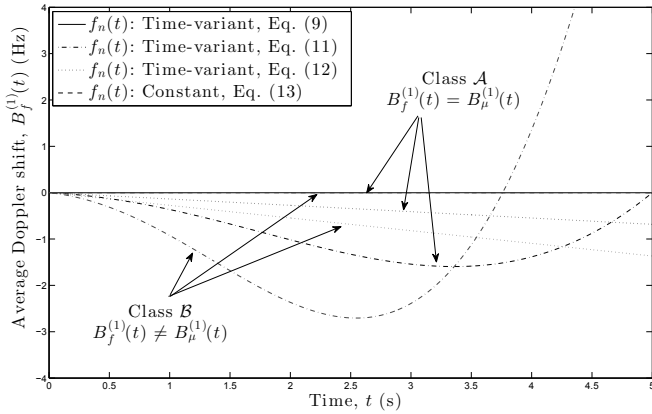


Fig. 2: Time-variant Doppler shifts $B_f^{(1)}(t)$ and $B_\mu^{(1)}(t)$ for the non-stationary multipath channel models of Class \mathcal{A} and Class \mathcal{B} .

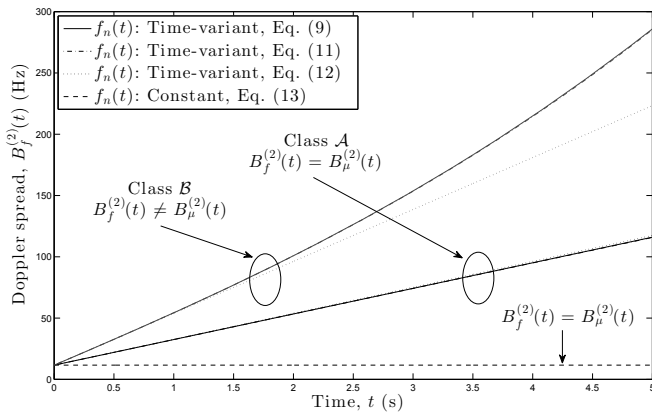


Fig. 3: Time-variant Doppler shifts $B_f^{(2)}(t)$ and $B_\mu^{(2)}(t)$ for the non-stationary multipath channel models of Class \mathcal{A} and Class \mathcal{B} .

a simple but effective method for computing stationary intervals by using the time-variant Doppler spread $B_f^{(2)}(t)$. The shortest time interval $T_q^{(2)}$ for which the absolute value of the relative error

$$\epsilon(T_q^{(2)}) = \frac{|B_f^{(2)}(T_q^{(2)}) - B_f^{(2)}(0)|}{B_f^{(2)}(0)} = \frac{q}{100} \quad (35)$$

equals q percent is called the stationary interval, where $B_f^{(2)}(0) \neq 0$. For the Class \mathcal{A} model, we obtain $T_5^{(2)} = 0.0278$ s, $T_{10}^{(2)} = 0.0556$ s, and $T_{20}^{(2)} = 0.1111$ s.

VII. CONCLUSION

In this paper, we have introduced two classes of non-stationary flat fading multipath channel models, which are termed Class \mathcal{A} and Class \mathcal{B} models. The Class \mathcal{A} models are obtained by computing the path phases of each multipath component via the integral over the corresponding time-variant

Doppler frequencies. The channel models of Class \mathcal{B} are based on standard wide-sense stationary SOC models, in which the time-invariant Doppler frequencies are replaced by time-variant Doppler frequencies. Three time-variant Doppler frequency models have been presented with different degrees of complexity; comprising an exact nonlinear model, an approximate nonlinear model, and a simple linear model. For any deterministic time-variant Doppler frequency process, it has been shown that the Class \mathcal{A} models are consistent w.r.t. both the time-variant average Doppler shift and the Doppler spread, whereas the non-stationary channel models of Class \mathcal{B} are inconsistent.

As the introduced consistency concept is physically sound and easy to apply, we believe that the study of this paper will have a great impact on future research directions regarding the development of non-stationary channel models. With the consistency concept under the belt, informed researchers will shift their focus from today's primarily studied Class \mathcal{B} models to the presented physically reasonable Class \mathcal{A} models.

REFERENCES

- [1] D. Umansky and M. Pätzold, "Stationarity test for wireless communication channels," in *Proc. IEEE Global Communications Conference, IEEE GLOBECOM 2009*. Honolulu, Hawaii, USA, Nov./Dec. 2009.
- [2] R. He *et al.*, "Characterization of quasi-stationarity regions for vehicle-to-vehicle radio channels," *IEEE Trans. Antennas Propag.*, vol. 63, no. 5, pp. 2237–2251, May 2015.
- [3] A. Ispas, C. Schneider, G. Ascheid, and R. Thomä, "Analysis of the local quasi-stationarity of measured dual-polarized MIMO channels," *IEEE Trans. Veh. Technol.*, vol. 64, no. 8, pp. 3481–3493, Aug. 2015.
- [4] R. Iqbal and T. D. Abhayapala, "Impact of mobile acceleration on the statistics of Rayleigh fading channel," in *Proc. 8th Australian Communication Theory Workshop, AusCTW 2007*. Adelaide, Australia, Feb. 2007, ISBN 1-4244-0741-9.
- [5] R. Iqbal, T. Abhayapal, J. Ahmed, and T. Lamahewa, "Wigner-Ville distribution of a type of non-stationary mobile Rayleigh fading channels," in *Proc. IEEE 13th International Multitopic Conference 2009, INMIC 2009*. Islamabad, Pakistan, Dec. 2009.
- [6] M. Pätzold and A. Borhani, "A non-stationary multipath fading channel model incorporating the effect of velocity variations of the mobile station," in *Proc. Wireless Communication and Network Conference, WCNC 2014*. Istanbul, Turkey, Apr. 2014, pp. 194–199.
- [7] W. Dahech, M. Pätzold, and N. Youssef, "A non-stationary mobile-to-mobile multipath fading channel model taking account of velocity variations of the mobile stations," in *Proc. 9th European Conference on Antennas and Propagation, EuCAP 2015*. Lisboa, Portugal, Apr. 2015.
- [8] S. Gligorevic, "Stochastic modeling of non-stationary channels," in *Proc. 7th European Conference on Antennas and Propagation, EuCAP 2013*. Gothenburg, Sweden, Apr. 2013.
- [9] X. Lia, X. Zhao, Y. Li, S. Li, and Q. Wang, "A non-stationary geometry-based street scattering model for vehicle-to-vehicle wideband MIMO channels," in *Proc. 26th IEEE Personal, Indoor and Mobile Radio Communications, PIMRC 2015*. Hong Kong, China, 2015, pp. 2239–2243.
- [10] B. Boashash, Ed., *Time-Frequency Signal Analysis and Processing: A Comprehensive Reference*, 2nd ed. Elsevier Academic Press, 2015.
- [11] B. O. Hogstad, C. A. Gutiérrez, M. Pätzold, and P. M. Crespo, "Classes of sum-of-cisoids processes and their statistics for the modelling and simulation of mobile fading channels," *EURASIP J. Wireless Commun. Netw.*, 2013, DOI 10.1186/1687-1499-2013-125.
- [12] M. Pätzold, *Mobile Radio Channels*, 2nd ed. Chichester: John Wiley & Sons, 2011.
- [13] M. Pätzold, B. O. Hogstad, and N. Youssef, "Modeling, analysis, and simulation of MIMO mobile-to-mobile fading channels," *IEEE Trans. Wireless Commun.*, vol. 7, no. 2, pp. 510–520, Feb. 2008.